Inorganic Chemistry

Article

pubs.acs.org/IC

A Twelve-Coordinated Iodide in a Cuboctahedral Silver(I) Skeleton

Jian-Hong Liao,[†] Camille Latouche,[‡] Bing Li,[§] Samia Kahlal,[‡] Jean-Yves Saillard,*[,‡] and C. W. Liu*[,†,§]

[†]Department of Chemistry, National Dong Hwa University, Hualien, Taiwan 97401, R. O. C.

[‡]UMR−CNRS, 6226 "Sciences Chimiques de Rennes", Université de Rennes 1, 35042 Rennes cedex, France

[§]Zhejiang Provincial Key Laboratory of Chemical Utilization of Forestry Biomass, Zhejiang A & F University, Lin'an, Zhejiang, 311300, P. R. China

Supporting Information

ABSTRACT: Three new halide-centered octanuclear silver(I) complexes, $[Ag_8(X)\{S_2P(CH_2CH_2Ph)_2\}_6](PF_6)$, X = F^-, **1**; Cl^-, **2**; Br^-, **3**; were prepared in the presence of the corresponding halide anions with silver(I) salts and dithiophosphinate ligands. Structure analyses displayed that a Ag_8 cubic core can be modulated by the size effect of the central halide; however, an iodide-centered Ag_8 cluster was not found under similar reaction conditions. Interestingly, a luminescent dodecanuclear silver(I) cluster, $[Ag_{12}(\mu_{12}\text{-I})(\mu_3\text{-I})_4\{S_2P(CH_2CH_2Ph)_2\}_6](I)$, **4**; was then synthesized. The structure of **4** contains a novel μ_{12}-I at the center of a cuboctahedral silver(I) atom cage, which is further stabilized by four additional μ_3-I and six dithiophosphinate ligands. To the best of our knowledge, the μ_{12}-I revealed in **4** is the highest coordination number for a halide ion authenticated by both experimental and computational studies. Previously, the μ_{12}-I was only observed in $[PyH][\{TpMo(\mu_3\text{-S})_4Cu_3\}_4(\mu_{12}\text{-I})]$. The synthetic details, spectroscopic studies including multinuclear NMR and ESI-MS, structure elucidations by single crystal X-ray diffraction, and photoluminescence of **4** are reported herein.

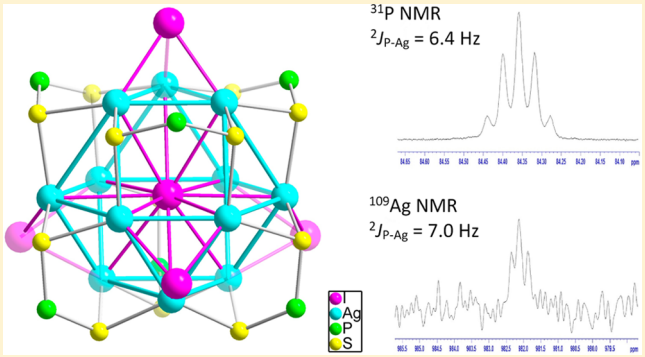

INTRODUCTION

The coordination number is widely used to describe the local chemical environments of a central atom in a molecule. Elements with high coordination numbers often violate the octet and the 18 electron rules and challenge chemists in the understanding of their bonding properties.[1] Debates on the nature of chemical bonding in elements with high coordination number have come along with the development of modern quantum chemistry.[2] How much is the highest possible coordination number of a main-group element? In the three-dimensional space, if all spheres are identical, this number is 12, corresponding to the theoretical limit of the kissing number problem, found in both hexagonal close-packed (HCP) and cubic close-packed (CCP).[3] It is also well-known that regular 12-vertex icosahedral structures are particularly stable and in some circumstances can accommodate a 12-coordinated atom in their center. Indeed, a few of examples with icosahedron such as $\{Au_{13}\}$ have been characterized by single crystal X-ray analysis and theoretical calculations.[4] The cuboctahedron has the same number of vertices, but its edges (24) are lower than those of an icosahedron (30). According to theoretical calculations, an M_{12} cuboctahedron has a higher energy than an M_{12} icosahedron.[5] Therefore, a discrete M_{13} cluster in a centered-cuboctahedral array has been rarely reported in the literature. There are two related crystal structures found in Cambridge Structural Database (v 5.34). One is a $Pt@Pt_{12}$ cuboctahedron edge-bridged by two additional Pt atoms and stabilized by carbonyl and phosphine ligands.[6] The other is a $Ag@Ag_{12}$ cuboctahedron with each trigonal face capped by Fe atoms and stabilized by carbonyl ligands.[7]

Like other main-group elements, halogens are subjects of high coordination such as in ClF_5 or ClF_7.[8] In order to explain the stability and bonding in such compounds, different theoretical treatments have been applied to rationalize and further to predict novel coordination modes for halogens.[9] This greatly promotes the development of the chemistry theories and guides people to synthesize new high-coordinated molecules. For years, the description of the structure and bonding in high-coordinated compounds was the strong participation of d orbitals. Nevertheless, there are several pieces of theoretical evidence that d-orbitals act as polarization functions, not true participants in hybridization.[10] So far, halogens have been shown to display various high coordination numbers and configurations.[11]

In recent years, our group has developed a chemistry of transition metal clusters with d^{10} electronic configuration and bridged by dichalcogenophosphate ligands $[E_2P(OR)_2^-$, E = S, Se]. Various high coordination numbers have been observed for halides located in the center of such clusters.[12] Rationalization

Received: November 30, 2013
Published: January 29, 2014

   dx.doi.org/10.1021/ic402960e | *Inorg. Chem.* 2014, 53, 2260−2267

of their bonding and stability has been provided by us.[13] In addition, we have found that the skeleton of the metallic cluster can change with the size and nature of the encapsulating ion.[12d] It is worthwhile to mention that three compounds, $[Ag_{11}(\mu_9\text{-}I)(\mu_3\text{-}I)_3\{E_2P(O^iPr)_2\}_6](PF_6)$ (E = S and Se),[11c] and $[Cu_{11}(\mu_9\text{-}Br)(\mu_3\text{-}Br)_3\{S_2P(O^iPr)_2\}_6](PF_6)$,[11d] containing a nonacoordinated halogen lying at the center of a M_{11} polyhedron, lead us to ponder whether this is the highest coordination number possible for halogen. Theoretically, one halogen can accommodate more than nine Cu^+ or Ag^+ in its periphery. In order to look for a larger coordination number for halogen, a new dithiophosphinate ligand, $[S_2P(CH_2CH_2Ph)_2]^-$, has been used to prepare novel transition metal clusters encapsulating a hypercoordinated main-group element. Herein, we report three new compounds, $[Ag_8(\mu_8\text{-}X)\{S_2P(CH_2CH_2Ph)_2\}_6](PF_6)$ (X = F, **1**; Cl, **2**; Br, **3**), and the first example of cuboctahedron Ag_{12} skeleton, $[Ag_{12}(\mu_{12}\text{-}I)(\mu_3\text{-}I)_4\{S_2P(CH_2CH_2Ph)_2\}_6](I)$ (**4**), with μ_{12}-iodide in the center by experimental and theoretical investigations.

RESULTS AND DISCUSSION

In a typical experiment (Scheme 1), the reaction of $[Ag(CH_3CN)_4](PF_6)$ with $(NH_4)[S_2P(CH_2CH_2Ph)_2]$ in an

Scheme 1. Synthetic Pathways for Compounds 1−4

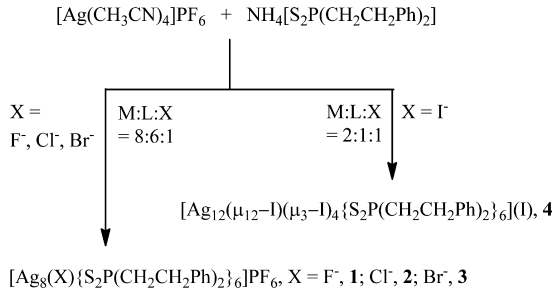

8:6 molar ratio for 10 min in THF solvent followed by the addition of 1 equiv of halide source under stirring leads to the formation of discrete halide-centered Ag^I_8 clusters **1**−**3**. By changing the metal to ligand ratio from 8:6 to 2:1 in methanol solvent, 1 equiv of Bu_4NI was added quickly into a mixture yielding to an iodide-centered Ag^I_{12} cuboctahedral cluster **4**. All four compounds were well characterized by multinuclear NMR spectroscopy, electrospray ionization mass spectroscopy, and X-ray crystallography. Compounds **1**−**3** crystallize in the space group $P(-)1$ with one molecule in the unit cell, and there are two acetone molecules co-crystallized in the lattice of compounds **1** and **3**. Their molecular structures are shown in Figure 1. The Ag_8XS_{12} core features a body-centered cube of approximate T_h symmetry,[12a] and each face is bridged by one dithiophosphinate ligand in a tetrametallic tetraconnective (μ_2, μ_2) coordination mode. Not taking into account the encapsulated X halogen, each silver ion is in an approximately trigonal-planar AgS_3 coordination mode and the AgS_3X coordination is of approximate trigonal pyramidal geometry. The Ag−X distances are in a range of 2.6657(3)−2.9116(3) Å (avg. 2.74(1) Å) in **1**, 2.8528(5)−2.9896(4) Å (avg. 2.88(8) Å) in **2**, and 2.883(1)−2.933(1) Å (avg. 2.91(3) Å) in **3**; the corresponding edge lengths of the Ag_8 cube are in the range of 3.0642(3)−3.2533(3) Å (avg. 3.16(7) Å) in **1**, 3.2190(5)−3.4136(5) Å (avg. 3.33(6) Å) in **2**, 3.323(2)−3.411(2) Å (avg. 3.36(3) Å) in **3**. The selected bond lengths and angles are listed in Table 1. The expansion of the Ag^I_8 cube is consistent with the increasing atomic radius from fluoride to bromide. However, one of the Ag−F distances in **1** is very long, 2.9116(3) Å, but it is still well within the range of appropriate sum of van der Waals radii. The Ag···Ag distances in the bromide-centered Ag^I_8 cage almost reach 3.44 Å, the sum of van der Waals radii of silver. Thus, it can be anticipated that the entrapment of the larger iodide into the Ag^I_8 cage would destabilize the structure.

Compound **4** crystallizes in the cubic space group $Pn(-)3m$ with two molecules in the unit cell. The counteranion, iodide, was found at the general position in the asymmetric unit but disordered in two positions. The cationic cluster of T_d symmetry (Figure 2) exhibits a $Ag_{12}(I)(I)_4$ core in which one iodide is encapsulated in a Ag_{12} cuboctahedron. It turns out that, as we were writing this paper, a similar coordination mode of iodide in a Cu(I) cuboctahedron was published.[11b] Therefore, our compound is the second example of a μ_{12}-I in cuboctahedral geometry, a coordination mode so far unique in main group chemistry. Four of the eight trigonal faces of the centered cuboctahedron are further capped by additional iodides, and each of the six "square" faces is bridged by a dithiophosphinate ligand in a (μ_2, μ_2) fashion, as those in compounds **1**−**3**. Each silver ion is in AgS_2I_2 coordination. Compared with the AgS_3Br fragment in **3** which is in a trigonal

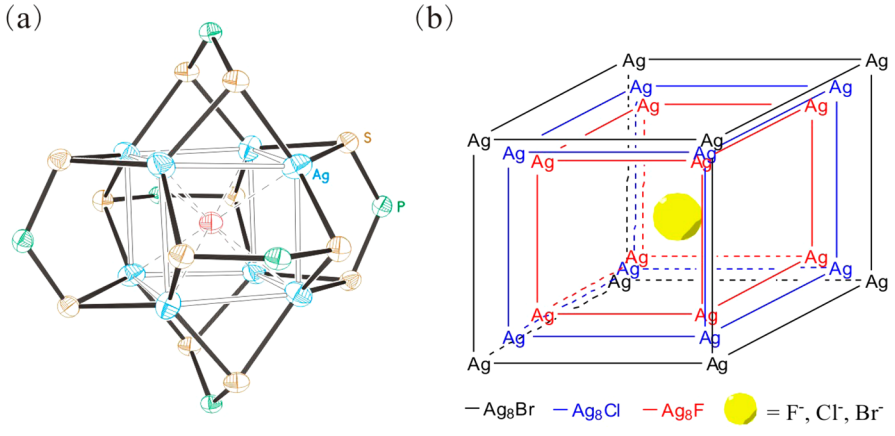

Figure 1. (a) Molecular structures of $[Ag_8(\mu_8\text{-}X)\{S_2P(CH_2CH_2Ph)_2\}_6]^+$ (30% thermal ellipsoid) with alkyl groups omitted for clarity. (b) Schematic representations of Ag_8 cubes with different interstitial halide anions.

dx.doi.org/10.1021/ic402960e | Inorg. Chem. 2014, 53, 2260−2267

Table 1. Selected Bond Lengths (Å) and Bond Angles (deg)

	1	2	3	4
Ag···Ag	3.0642(3)−3.2533(3) avg. 3.16(7)	3.2190(5)−3.4136(5) avg. 3.33(6)	3.323(2)−3.411(2) avg. 3.36(3)	3.111(2)
Ag−X_{center}	2.6657(3)−2.9116(3)	2.8528(5)−2.9896(4)	2.883(1)−2.933(1)	3.380(1)
Ag−X_{cap}	−	−	−	2.810(2)
P−S	2.025(1)−2.036(1)	2.025(2)−2.036(2)	2.016(7)−2.04(1)	1.999(4)
S−Ag	2.4884(7)−2.5413(8)	2.469(1)−2.549(1)	2.498(4)−2.536(4)	2.491(3)
S−P−S	119.00(5)−119.36(4)	119.90(7)−120.19(7)	120.9(4)−121.3(2)	120.2(3)
Ag−S−Ag	74.64(2)−80.87(2)	78.83(4)−85.16(4)	82.4(2)−85.8(1)	93.9(1)

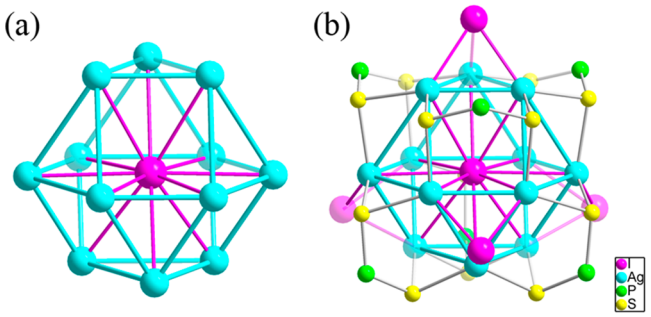

Figure 2. (a) A μ_{12}-I-centered cuboctahedral Ag^{I}_{12} skeleton in compound **4** (30% thermal ellipsoid). (b) Molecular structure of $[Ag_{12}(\mu_{12}\text{-}I)(\mu_3\text{-}I)_4\{S_2P(CH_2CH_2Ph)_2\}_6]^+$ with alkyl groups omitted for clarity.

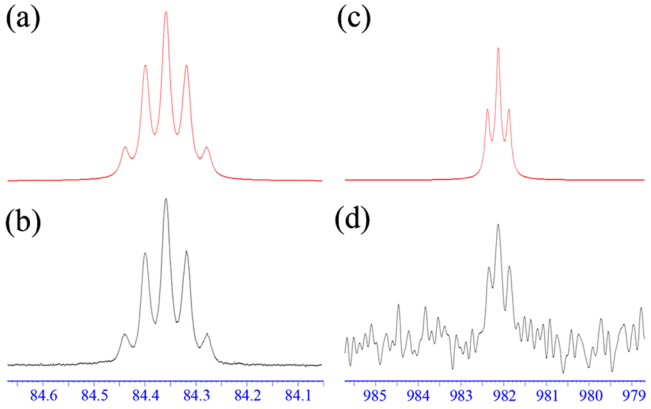

Figure 3. (a) Simulated $^{31}P\{^1H\}$ NMR spectrum and (b) experimental data of compound **4**. (c) Simulated $^{109}Ag\{^1H\}$ NMR spectrum and (d) experimental data of compound **4**.

pyramidal geometry, the sum of the bond angles around silver indicates that the coordination geometry of the AgS_2I_2 fragment is approximately tetrahedral. The distance of silver to central iodide, 3.380(1) Å, is much longer than the Ag−μ_3-I distance of 2.810(2) Å. This reflects the strong bonding interactions between the capping iodides and silver atoms of the trigonal faces. The shortest Ag···Ag distances (3.111(2) Å) also appear at the edges of the trigonal faces. The whole structure can also be represented as four Ag_3I units, connected together in tetrahedral arrangement via six dithiophosphinate ligands and a central iodide anion. The hypercoordinated iodide might play a role in self-assembly synthesis.

The $^{31}P\{^1H\}$ NMR spectrum of compounds **1**−**3** displays a quintet peak around 82 ppm. The molecular structures having T_h symmetry in compounds **1**−**3** have six ligands bridging on the square face, and each connects to four silver atoms, which are magnetically equivalent. This quintet is the result of a typical two-bond $^{31}P-^{109}Ag(^{107}Ag)$ coupling ($^2J_{PAg}$ = 6.0 Hz). The central fluoride in **1** was also characterized by ^{19}F NMR with a resonance frequency at −151.2 ppm. This value is within the range of typical octanuclear metal clusters with an encapsulated fluoride anion, such as −152.5 ppm for $[Cu_8(F)\{Se_2P(O^iPr)_2\}_6]PF_6$[12b] and −150.5 ppm for $[Ag_8(F)\{S_2P(OEt)_2\}_6]PF_6$,[12e] but is significantly upfield-shifted in comparison with δ −65.7 ppm for $[Ag_{14}(C{\equiv}C^tBu)_{12}(F)](BF_4)$.[14] In the $^{31}P\{^1H\}$ NMR spectrum of compound **4**, a distinct quintet peak around 84.4 ppm ($^2J_{PAg}$ = 6.4 Hz) corresponds to the resonance of dithiophosphinate ligand capped on the square face formed by four silver atoms of the cuboctahedron. All ligands are magnetically equivalent due to interchanges by T_d symmetry, as are the twelve silver atoms. Thus, a triplet peak was observed at 982.0 ppm in the $^{109}Ag\{^1H\}$ NMR spectrum that corresponds to each tetrahedrally coordinated AgS_2I_2 silver. The simulated ^{31}P and ^{109}Ag NMR spectra which match well with the experimental data are depicted in Figure 3. The positive ESI-MS spectrum of compound **4** (Figure 4) displays a major peak around 3757.5 (m/z) which corresponds to the molecular ion of $[Ag_{12}(I)_5\{S_2P(CH_2CH_2Ph)_2\}_6]^+$. Its theoretically determined isotopic pattern shows excellent agreement with the experimental one (Figure 4 inset). Within this range, a calculated fragment peak at 2822.4 (m/z) which corresponds to $[Ag_8(I)\{S_2P(CH_2CH_2Ph)_2\}_6]^+$ was not found. Thus, it provides indirect evidence that the formation of the iodide-centered Ag_8 skeleton is not possible even in the gas phase, andcan be attributed to the size effect of the iodide.

Density functional theory (DFT) calculations have been carried out on the model $[Ag_{12}(\mu_{12}\text{-}I)(\mu_3\text{-}I)_4(S_2PH_2)_6]^+$ (**4′**) using several functionals with the Def2-TZVP basis set for geometry optimizations (see Computational Details). We describe below the results obtained at the BP86 level for which an overall good structural consistency was found with the X-ray structure. The optimized Ag−μ_{12}-I (3.48 Å) distance is slightly overestimated with respect to the experimental one, whereas the Ag−μ_3-I one (2.82 Å) nears the X-ray value. Similarly, the shortest Ag−Ag distance (3.07 Å) is close to its X-ray counterpart, whereas the largest one (3.87 Å) is slightly overestimated. The existence of twelve Ag−μ_{12}-I bonding contacts is proven by the corresponding Ag−I Wiberg indices, the sum of which is 0.410. This value can be compared to the sum of the three Ag−μ_3-I Wiberg indices (0.765). It can also be compared to the corresponding values associated with the encapsulated iodine calculated at the same level of theory for the hypothetical cubic model $[Ag_8(\mu_8\text{-}I)(S_2PH_2)_6]^+$ (0.416) and for $[Ag_{11}(\mu_9\text{-}I)(\mu_3\text{-}I)_3\{S_2P(OH)_2\}_6]^+$ (0.410), a model for $[Ag_{11}(\mu_9\text{-}I)(\mu_3\text{-}I)_3\{S_2P(O^iPr)_2\}_6]^+$.[11c] In these two latter clusters, the NBO charge of the central iodine is −0.77 and −0.74, respectively. It is −0.70 in **4′**. These data are consistent with the existence of a significant covalent component in the bonding between the encapsulated iodide and its guest cage in

dx.doi.org/10.1021/ic402960e | Inorg. Chem. 2014, 53, 2260−2267

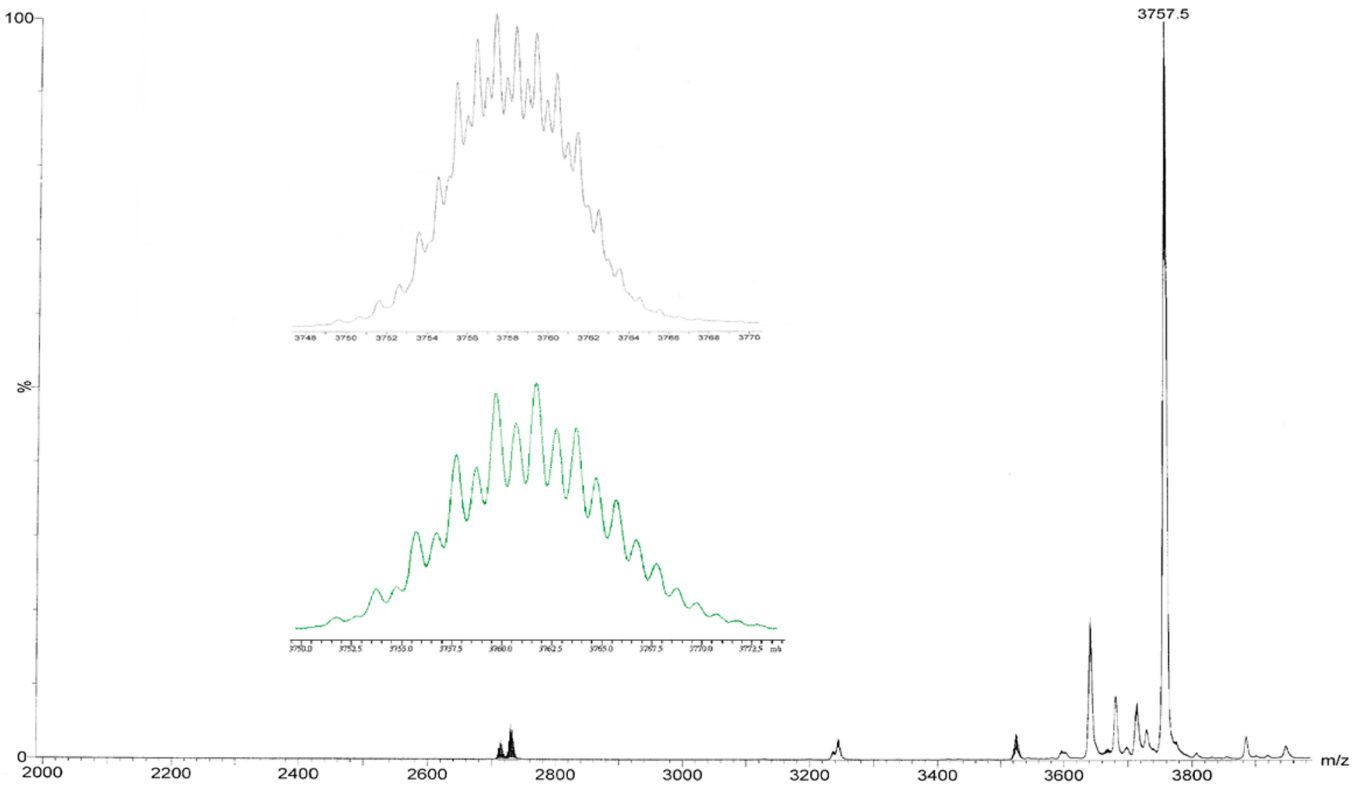

Figure 4. Positive ESI-mass spectrum of **4**: the experimental isotopic pattern (top left) centered at 3757.5 (m/z) and the simulated isotopic pattern for $[Ag_{12}(I)_5\{S_2P(CH_2CH_2Ph)_2\}_6]^+$ at bottom left.

Table 2. Relevant Computed Data for $[Ag_{12}(\mu_{12}\text{-}X)(\mu_3\text{-}I)_4(S_2PH_2)_6]^+$ (4′) and $[Ag_8(\mu_8\text{-}X)(S_2PH_2)_6]^+$[a]

		X = I	X = Br	X = Cl
$[Ag_{12}(\mu_{12}\text{-}X)(\mu_3\text{-}I)_4(S_2PH_2)_6]^+$	X natural orbital charge and populations	−0.70 ($5s^{1.96}$ $5p^{5.74}$ $5d^{0.01}$)	−0.73 ($4s^{1.97}$ $4p^{5.76}$)	−0.73 ($3s^{1.97}$ $3p^{5.75}$)
	Ag-X Wiberg index	0.034	0.030	0.030
	BE	7.59	7.71	7.91
	DE	7.30	7.38	7.55
	ΔE_{dist}	0.29	0.32	0.36
$[Ag_8(\mu_8\text{-}X)(S_2PH_2)_6]^+$	X natural orbital charge and populations	−0.77 ($5s^{1.95}$ $5p^{5.80}$ $5d^{0.01}$)	−0.81 ($3s^{1.94}$ $3p^{5.86}$)	−0.82 ($4s^{1.94}$ $4p^{5.86}$)
	Ag-X Wiberg index	0.052	0.041	0.038
	BE	6.73	7.78	8.24
	DE	6.49	7.65	8.13
	ΔE_{dist}	0.24	0.13	0.11

[a]Energies are in eV.

4′ and with the fact that covalency does not decrease when the iodide coordination number increases.

As mentioned above, $[Ag_8(X)\{S_2P(CH_2CH_2Ph)_2\}_6]^+$ (X = halogen) could not be isolated in the case of iodine, whereas the lighter halogens did not lead to the formation of the dodecanuclear species $[Ag_{12}(\mu_{12}\text{-}X)(\mu_3\text{-}I)_4\{S_2P(CH_2CH_2Ph)_2\}_6]^+$. Actually, no hexa(dichalcogeno) octanuclear Cu(I) or Ag(I) cluster containing an encapsulated iodine is known, whereas there are many examples containing an encapsulated fluorine, chlorine, or bromine atom.[12d] In order to get a better insight into this experimental fact, we have calculated the two model series $[Ag_8(\mu_8\text{-}X)(S_2PH_2)_6]^+$ and $[Ag_{12}(\mu_{12}\text{-}X)(\mu_3\text{-}I)_4(S_2PH_2)_6]^+$ for X = I, Br, and Cl. The major computed data are reported in Table 2, in which BE is the bonding energy between X^- and its host cage, defined as the absolute value of the difference between the energy of the halogen-containing cluster in its equilibrium geometry and the sum of the energies of X^- and of the empty cage in the frozen geometry it adopts in the halogen-containing cluster. DE is the dissociation energy calculated in the same way as BE except that the empty cage is considered in its (relaxed) equilibrium geometry. Thus, the difference between BE and DE is simply the amount of energy required to distort the relaxed empty cage into the geometry it adopts in the halogen-containing cluster (ΔE_{Dist}), i.e., DE = BE − ΔE_{Dist}. From the BE and DE values of Table 2, one can see that the encapsulation of iodine in an octanuclear cage is clearly disfavored. Thus, whereas $[Ag_8(\mu_8\text{-}I)(S_2PR_2)_6]^+$ is a minimum on the potential energy surface, its formation is thermodynamically strongly disfavored with respect to that of its dodecanuclear relative **4′**. The opposite trend is found for bromine and chlorine for which encapsulation in an octanuclear cluster is favored. However, this preference for octacoordination is not as strong as that for dodecacoordination in the case of iodine, especially for

dx.doi.org/10.1021/ic402960e | Inorg. Chem. 2014, 53, 2260−2267

bromine. Clearly, this is the size effect which is at work, the larger iodine preferring larger host cages. For comparison, the BE value computed for $[Ag_{11}(\mu_9\text{-I})(\mu_3\text{-I})_3\{Se_2P(OH)_2\}_6]^+$ is 7.68 eV,[11c] a value close to that computed for **4**′ (7.59 eV). One should note that this high coordination preference is not related to any significant participation of the 5d(I) orbitals (see Table 2).[15]

Photophysical data for compound **4** in the solid and solution states at 298 and 77 K are summarized in Table 3, and spectra

Table 3. Photophysical Data for 4

state (T/K)	λ_{abs}/nm (ε/dm^3 mol^{-1} cm^{-1})	$\lambda_{ex.}$(nm)	$\lambda_{em.}$ (nm)	life time (μs)
CH_2Cl_2 (298)	282 (14500), 323 (15700), 427 (7100)	436	533	
CH_2Cl_2 (77)		336, 420	556	
Solid (298)		450	533	0.75
Solid (77)		444	560	47.1, 17.0

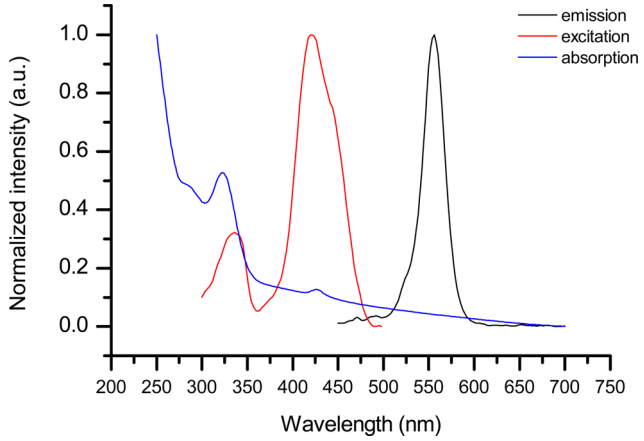

Figure 5. Normalized excitation (red) and emission (black) spectra in CH_2Cl_2 at 77K of **4**. Electronic absorption spectrum (blue line) in CH_2Cl_2 at ambient temperature.

at 77 K in CH_2Cl_2 are shown in Figure 5. The complex displays a yellow luminescence under UV irradiation with the emission lifetime in microsecond range. Upon lowering temperature, a small red shift at emission maxima was observed in both solid and solution. It exhibits intense absorption at 282 and 323 nm with large extinction coefficient of $\sim 10^4$ dm^3 mol^{-1} cm^{-1}, indicating a fully allowed charge-transfer transition. Additionally, a low-energy band was observed at 427 nm which was also found in $[Ag_{11}(\mu_9\text{-X})(\mu_3\text{-I})_3\{E_2P(O^iPr)_2\}_6](PF_6)$, X = I, E = S, Se;[11c] X = Se, E = Se.[16a]

TDDFT calculations performed on **4**′ at the PBE0/LANL2DZ+pol level on the previously optimized geometry found the two absorption transitions of lowest energy at 316 and 296 nm. The first one can be described as a $3t_2 \rightarrow 1a_1$ transition (92%) and the second one as the $2t_2 \rightarrow 1a_1$ (78%) (see the MO diagram and compositions of **4**′ in Figure 6). The highest occupied MO's are a mixture of 4d(Ag) AO's with μ_3-I and S lone pairs, with some μ_{12}-I admixture in the case of levels of t_2 symmetry. As in many polynuclear Cu(I) and Ag(I) clusters stabilized by dichalcogeno ligands, the LUMO is largely composed of metal valence 5p and 5s orbitals, mixed in a

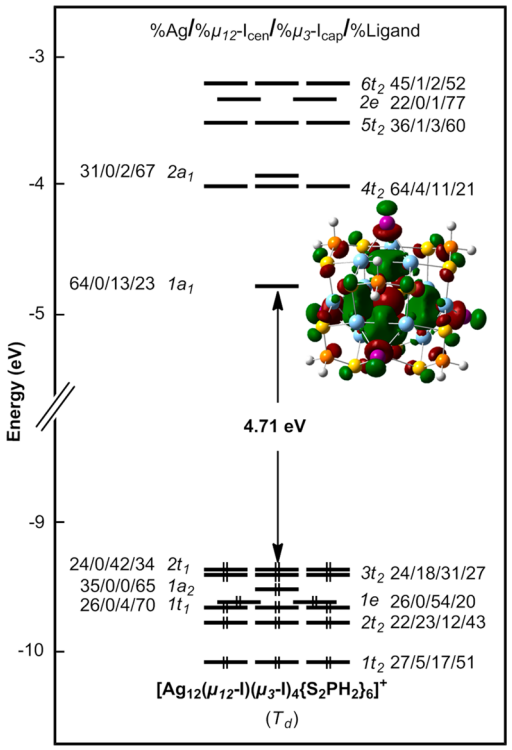

Figure 6. MO diagram of **4**′ at the PBE0/LANL2DZ+pol. level of theory.

bonding way.[16b] This is its bonding character which tends to somehow isolate this $1a_1$ LUMO from the other unoccupied orbitals which are mainly metal−ligand antibonding. The charge reorganization afforded upon these two transitions is quite complex. The $3t_2 \rightarrow 1a_1$ transition is mainly of XMCT character (X = μ_{12}-I and μ_3-I) mixed some M(4d)M(5p +5s)CT. The $2t_2 \rightarrow 1a_1$ transition is mainly LMCT and XLCT (X = μ_{12}-I) in character, mixed also with some M(4d)M(5p +5s)CT.

CONCLUSIONS

Structural analyses of three halide-centered Ag_8 cubes **1**−**3** strongly suggest that Ag···Ag edge lengths of the anion-centered cubic Ag_8 core are consistent with the radius of halides encapsulated at the center. Interestingly, compound **4** has a rare cuboctahedral Ag_{12} framework of which four of the eight trigonal faces of the cuboctahedron are further capped by additional iodides and each of the six square faces is bridged by a dithiophosphinate ligand. As a result, compound **4** has an idealized T_d symmetry. Indeed, the symmetry displayed in the solid state is retained in solution as evidenced by the distinct coupling patterns revealed from both ^{31}P and ^{109}Ag NMR spectroscopy. Furthermore, an iodide inscribed at the center of a dodecanuclear silver cluster exhibits strong covalent interactions with peripheral silver atoms and shows an unprecedented cuboctahedral coordination environment for a main-group element. To the best of our knowledge, μ_{12}-I revealed in **4** is the highest coordination number of any main group element authenticated by both experimental and computational studies. In addition, the cluster **4** exhibits a strong yellow emission under UV irradiation whereas halide-centered Ag_8 cubic clusters **1**−**3** do not luminesce even at 77 K.

dx.doi.org/10.1021/ic402960e | Inorg. Chem. 2014, 53, 2260−2267

Table 4. Selected X-ray Crystallographic Data for Compounds 1−4

	1·2[$(CH_3)_2CO$]	2·2[$(CH_3)_2CO$]	3	4
formula	$C_{96}H_{108}Ag_8F_7P_7S_{12}$·2[$(CH_3)_2CO$]	$C_{96}H_{108}Ag_8ClF_6P_7S_{12}$·2[$(CH_3)_2CO$]	$C_{96}H_{108}Ag_8BrF_6P_7S_{12}$	$C_{96}H_{108}Ag_{12}I_6P_6S_{12}$
formula weight	2975.45	2991.90	2920.20	3888.20
crystal system	triclinic	triclinic	triclinic	cubic
space group	$P(-)1$	$P(-)1$	$P(-)1$	$Pn(-)3m$
a, Å	14.0927(9)	14.0917(8)	12.7022(18)	18.2949(7)
b, Å	14.7542(9)	14.7983(9)	15.623(2)	18.2949(7)
c, Å	15.6330(9)	15.6099(9)	15.907(2)	18.2949(7)
α, deg	65.7230(10)	65.5480(10)	64.959(2)	90
β, deg	84.2270(10)	84.3080(10)	86.766(3)	90
γ, deg	76.2210(10)	76.1070(10)	79.957(3)	90
V, Å^3	2877.8(3)	2876.5(3)	2815.5(7)	6123.4(4)
Z	1	1	1	2
ρ_{calcd}, g cm^{-3}	1.717	1.727	1.722	2.109
μ, mm^{-1}	1.703	1.725	2.089	3.708
T, K	296(2)	296(2)	100(2)	296(2)
reflections collected	27957	27135	24105	25136
independent reflections	11839 (R_{int} = 0.0227)	11764 (R_{int} = 0.0224)	9898 (R_{int} = 0.0260)	1042 (R_{int} = 0.0292)
θ_{max}, deg/completeness, %	26.47/99.5	26.40/99.5	25.00/99.8	24.99/100.0
$R1^a$, $wR2^b$ [I > 2σ(I)]	0.0296, 0.0860	0.0406, 0.0850	0.0957, 0.2189	0.0683, 0.2080
$R1^a$, $wR2^b$ (all data)	0.0345, 0.0894	0.0563, 0.0946	0.1167, 0.2370	0.0844, 0.2501
Goodness-of-fit	1.037	1.056	1.048	1.112
largest diff. peak and hole, e/ Å^3	0.980, −0.529	1.160, −0.554	2.568, −2.477	2.663, −0.584

$^a R1 = \Sigma||F_o|-|F_c||/\Sigma|F_o|$. $^b wR2 = \{\Sigma[w(F_o^2-F_c^2)^2]/\Sigma[w(F_o^2)^2]$.

EXPERIMENTAL SECTION

All solvents were purified following standard protocols.[17] All reactions were performed in oven-dried Schlenk glassware by using standard inert-atmosphere techniques. The ligand, $NH_4[S_2P(CH_2CH_2Ph)_2]$, was prepared according to the literature methods.[18] Other chemicals were purchased from commercial sources and used as received. Melting point was determined with a Fargo MP-2D apparatus. The elemental analyses were done using a Perkin-Elmer 2400 CHN analyzer. NMR spectra were recorded on a Bruker Advanced DPX300 FT-NMR spectrometer, which operates at 300 MHz while recording ^{1}H, 121.49 MHz while recording ^{31}P. ^{19}F NMR spectra were recorded on a Bruker Avance II 400 spectrometer operating at 376.5 MHz. ^{109}Ag{^{1}H} NMR spectrum was recorded on a Bruker 600 UltraShield spectrometer operating at 28 MHz. UV−vis spectra were recorded on a Lamdba 750 UV/vis spectrometer. Luminescence measurements were done on a Edinburgh FLSP920 spectrometer, equipped with an Oxford cryostat (OptistatDN) and a digital temperature controller.

Synthesis of $[Ag_8(\mu_8\text{-}F)\{S_2P(CH_2CH_2Ph)_2\}_6]PF_6$ (1). $[Ag(CH_3CN)_4]PF_6$ (0.086 g, 0.206 mmol) and $NH_4[S_2P(CH_2CH_2Ph)_2]$ (0.050 g, 0.155 mmol) were added in Schlenk flask; 30 mL of THF was added and kept stirring under N_2 atmosphere at room temperature for 10 min. Bu_4NF (0.007 g, 0.026 mmol) was following added and kept under continuous stirring for 3 h. The reaction mixture was then filtered to get rid of any solid, and the filtrate was evaporated to dryness under vacuum to give a beige powder, washed with a large amount of methanol, followed with deionized water. Yield: 40.7% (0.030 g). M.p.: 279 °C. Anal. Calcd. for $C_{96}H_{108}Ag_8F_7P_7S_{12}$: C 40.32; H 3.81. Found: C 40.06; H 4.02. ^{1}H NMR (300 MHz, acetone-d_6): 2.52 (*m*, 24H, CH_2Ph), 3.05 (*m*, 24H, PCH_2), 7.22 (*m*, 60H, C_6H_5) ppm. ^{31}P{^{1}H} NMR (121.49 MHz, $CDCl_3$): 81.9 (*q*, $^2J_{PAg}$ = 6.0 Hz, PS_2), −143.0 (*sept.*, J_{PF} = 712.0 Hz, PF_6) ppm. ^{19}F NMR (376.5 MHz, $CDCl_3$): −151.2 (*s*, Ag_8F), −71.7 (*d*, J_{PF} = 708.0 Hz, PF_6) ppm. ESI−MS (*m*/*z*) calcd. for $[Ag_8(F)\{S_2P(CH_2CH_2Ph)_2\}_6]^+$: 2714.6. Found: 2714.7.

The synthesis is general to compounds **2**−**4** by replacing Bu_4NF with equimolar $BzEt_3NCl$ and PPh_4Br, respectively.

$[Ag_8(\mu_8\text{-}Cl)\{S_2P(CH_2CH_2Ph)_2\}_6]PF_6$ (2). Yield: 72.5% (0.054 g). M.p.: 261 °C. Anal. Calcd. for $C_{96}H_{108}Ag_8ClF_6P_7S_{12}$: C 40.09; H 3.79. Found: C 40.21; H 3.98. ^{1}H NMR (300 MHz, acetone-d_6): 2.54 (*m*, 24H, CH_2Ph), 2.98 (*m*, 24H, PCH_2), 7.22 (*m*, 60H, C_6H_5) ppm. ^{31}P{^{1}H} NMR (121.49 MHz, $CDCl_3$): 82.1 (*q*, $^2J_{PAg}$ = 6.0 Hz, PS_2), −143.0 (*sept.*, J_{PF} = 712.0 Hz, PF_6) ppm. ESI−MS (*m*/*z*) calcd. for $[Ag_8(Cl)\{S_2P(CH_2CH_2Ph)_2\}_6]^+$: 2730.6. Found: 2731.2.

$[Ag_8(\mu_8\text{-}Br)\{S_2P(CH_2CH_2Ph)_2\}_6]PF_6$ (3). Yield: 60.3% (0.045 g). M.p.: 257 °C. Anal. Calcd. for $C_{96}H_{108}Ag_8BrF_6P_7S_{12}$: C 39.48; H 3.73. Found: C 39.80; H 3.88. ^{1}H NMR (300 MHz, acetone-d_6): 2.56 (*m*, 24H, CH_2Ph), 3.07 (*m*, 24H, PCH_2), 7.22 (*m*, 60H, C_6H_5) ppm. ^{31}P{^{1}H} NMR (121.49 MHz, $CDCl_3$): 81.9 (*q*, $^2J_{PAg}$ = 6.0 Hz, PS_2), −143.0 (*sept.*, J_{PF} = 712.0 Hz, PF_6) ppm. ESI−MS (*m*/*z*) calcd. for $[Ag_8(Br)\{S_2P(CH_2CH_2Ph)_2\}_6]^+$: 2774.5. Found: 2774.2.

$[Ag_{12}(\mu_{12}\text{-}I)(\mu_3\text{-}I)_4\{S_2P(CH_2CH_2Ph)_2\}_6](I)$ (4). $[Ag(CH_3CN)_4]PF_6$ (0.129 g, 0.309 mmol), $NH_4[S_2P(CH_2CH_2Ph)_2]$ (0.050 g, 0.155 mmol) and Bu_4NI (0.057 g, 0.155 mmol) were added in the Schlenk flask, 30 mL of methanol was added and kept stirring under N_2 atmosphere at room temperature for 5 h. The precipitate was collected from the yellow suspension and then evaporated to dryness under vacuum. It was washed with large amount of methanol, followed by deionized water to get a yellow powder. Yield: 62.7% (0.063 g). M.p.: 253 °C. Anal. Calcd. for $C_{96}H_{108}Ag_{12}I_6P_6S_{12}$·3$H_2O$: C 29.25; H 2.91. Found: C 28.87; H 2.90. ^{1}H NMR (300 MHz, acetone-d_6): 2.71 (*m*, 24H, CH_2Ph), 2.98 (*m*, 24H, PCH_2), 7.25 (*m*, 60H, C_6H_5) ppm. ^{31}P{^{1}H} NMR (121.49 MHz, $CDCl_3$): 84.4 (*q*, $^2J_{PAg}$ = 6.4 Hz, PS_2) ppm. ^{109}Ag{^{1}H} NMR (28.0 MHz, $CDCl_3$): 982.0 (*t*, $^2J_{PAg}$ = 7.0 Hz) ppm. ESI−MS (*m*/*z*) calcd. for $[Ag_{12}(I)_5\{S_2P(CH_2CH_2Ph)_2\}_6]^+$: 3759.7. Found: 3757.5.

X-ray Structure Analysis. Single crystals of **1**, **2**, and **3** were grown by slowly diffusing hexane into acetone solution at ambient temperature. Colorless crystals were formed within one week. Single crystals of **4** were grown by using the same method with chloroform solution instead of acetone. Yellow crystals were formed after two weeks. All reflection data were collected on a Bruker SMART APEX-II CCD instrument by using graphite monochromatic Mo Kα radiation (λ = 0.71073 Å). A semiempirical absorption correction by using SADABS was applied, and the raw data frame integration was performed with SAINT.[19] Structures were solved by direct method and were refined against the least-squares methods on F^2 with the SHELXL-97 package,[20] incorporated in SHELXTL-PC v 5.10.[21] All non-hydrogen atoms were refined anisotropically. The detailed refinements were written in the "refine_special_details" part in cif.

dx.doi.org/10.1021/ic402960e | Inorg. Chem. 2014, 53, 2260−2267

CCDC 949774–949777 (**1**–**4**) contains the supplementary crystallographic data for this paper. Selected crystallographic data of compounds **1**–**4** are listed in Table 4.

Computational Details. Density functional theory (DFT) geometry optimizations have been carried out on **4′**, using the Gaussian 09 package,[22] with the Def2-TZVP (triple-ζ polarized) basis set from the EMSL Basis Set Exchange Library.[23] After testing several functionals (BP86,[24] M06,[25] M06L,[26] PBE0,[27] BP7D[28]) the BP86 functional has been selected for giving the best agreement between the optimized geometry of **4′** and the X-ray structure of **4** (see Table 5). All the stationary points were fully characterized as true minima via analytical frequency calculations.

Table 5. Relevant Computed Interatomic Bond Distances (Å) for Optimized Structures of 4′, Using Different Functionals

	X-ray	BP86	M06	M06L	PBE0	B97D
Ag1–Ag2	3.111	3.070	3.050	2.983	3.135	3.435
Ag1–Ag3	3.640	3.873	3.908	3.849	3.865	3.661
Ag-μ_{12}–I	3.380	3.483	3.492	3.429	3.510	3.549
Ag-μ_3–I	2.810	2.820	2.819	2.868	2.796	2.874

The natural orbital analysis was performed with the NBO 5.0 program.[29] The composition of the molecular orbitals and the Wiberg indices were calculated using the AOMix program.[30] Single-point time dependent DFT (TD-DFT) calculations were performed on the optimized BP86/Def2-TZVP geometry of **4′** with the PBE0 functional[27] and the LANL2DZ+pol. basis set.[31]

■ ASSOCIATED CONTENT

Supporting Information

Crystallographic data (CIF) for compounds **1**–**4**. Atomic Cartesian coordinates and total energy of the computed models. This material is available free of charge via the Internet at http://pubs.acs.org.

■ AUTHOR INFORMATION

Corresponding Author

*E-mail: chenwei@ndhu.edu.edu.tw.

Notes

The authors declare no competing financial interest.

■ ACKNOWLEDGMENTS

This work was supported by the National Science Council of Taiwan (NSC 100-2113-M-259-003). J.-Y.S. thanks the Institut Universitaire de France for support. We thank Dr. Y.-Y. Wu for the simulated NMR spectra.

■ REFERENCES

(1) (a) Galeev, T. R.; Romanescu, C.; Li, W.-L.; Wang, L.-S.; Boldyrev, A. I. *Angew. Chem., Int. Ed.* **2012**, *51*, 2101. (b) Hermann, A.; Lein, M.; Schwerdtfeger, P. *Angew. Chem., Int. Ed.* **2007**, *46*, 2444. (c) Daly, S. R.; Piccoli, P. M. B.; Schultz, A. J.; Todorova, T. K.; Gagliardi, L.; Girolami, G. S. *Angew. Chem., Int. Ed.* **2010**, *49*, 3379. (d) Gillespie, R. J.; Silvi, B. *Coord. Chem. Rev.* **2002**, *233–234*, 53.

(2) (a) Leiding, J.; Woon, D. E.; Dunning, T. H. *J. Phys. Chem. A* **2011**, *115*, 4757. (b) Vedha, S. A.; Solomon, R. V.; Venuvanalingam, P. *J. Phys. Chem. A* **2013**, *117*, 3529. (c) Borissova, A. O.; Lyssenko, K. A. *Mendeleev Commun.* **2011**, *21*, 160. (d) Ito, K.; Pu, Z. F.; Li, Q. S.; Schleye, P. R. *Inorg. Chem.* **2008**, *47*, 10906. (e) Cui, Z.-H.; Contreras, M.; Ding, Y.-H; Merino, G. *J. Am. Chem. Soc.* **2011**, *133*, 13228. (f) Islas, R.; Heine, T.; Ito, K.; Schleyer, P. R.; Merino, G. *J. Am. Chem. Soc.* **2007**, *129*, 14767.

(3) West, A. R. *Basic Solid State Chemistry*, 2nd ed.; John Wiley & Sons Ltd: New York, 1999.

(4) (a) Briant, C. E.; Theobald, B. R. C.; White, J. W.; Bell, L. K.; Mingos, D. M. P. *J. Chem. Soc. Chem. Commun.* **1981**, 201. (b) Qian, H.; Eckenhoff, W. T.; Zhu, Y.; Pintauer, T.; Jin, R. *J. Am. Chem. Soc.* **2010**, *132*, 8280. (c) Wan, X.-K.; Lin, Z.-W.; Wang, Q.-M. *J. Am. Chem. Soc.* **2012**, *134*, 14750. (d) Yang, C.-L.; Wang, M.-S.; Sun, M.-Y.; Wang, D.-H.; Ma, X.-G.; Gong, Y.-B. *Chem. Phys. Lett.* **2008**, *457*, 49.

(5) Zhao, G.-F.; Wang, Y.-L.; Sun, J.-M.; Wang, Y.-X. *Acta Phys.-Chim. Sin.* **2012**, *28*, 1355.

(6) Howard, J. A. K.; Spencer, J. L.; Turner, D. G. *J. Chem. Soc., Dalton. Trans.* **1987**, 259.

(7) Albano, V. G.; Grossi, L.; Longoni, G.; Monari, M.; Mulley, S.; Sironi, A. *J. Am. Chem. Soc.* **1992**, *114*, 5708.

(8) (a) Thanthiriwatte, K. S.; Vasiliu, M.; Dixon, D. A.; Christe, K. O. *Inorg. Chem.* **2012**, *51*, 10966. (b) Law, C.-K.; Chien, S.-H.; Li, W.-K.; Cheung, Y.-S. *J. Phys. Chem. A* **2002**, *106*, 11271. (c) Chen, L.; Woon, D. E.; Dunning, T. H. *J. Phys. Chem. A* **2009**, *113*, 12645. (d) Schroer, T.; Christe, K. O. *Inorg. Chem.* **2001**, *40*, 2415.

(9) (a) Dobado, J. A.; Martínez-García, H.; Molina, J. M.; Sundberg, M. R. *J. Am. Chem. Soc.* **1999**, *121*, 3156. (b) Lee, T. J. *J. Phys. Chem.* **1994**, *98*, 3697. (c) Chen, L.; Woon, D. E.; Dunning, T. H. *J. Phys. Chem. A* **2009**, *113*, 12645.

(10) Curnow, O. J. *J. Chem. Educ.* **1998**, *75*, 910.

(11) (a) Wang, R.; Jin, T.; Zhang, Z.; Staples, R. J. *Angew. Chem., Int. Ed.* **1999**, *38*, 1813. (b) Wei, Z.-H.; Ni, C.-Y.; Li, H.-X.; Ren, Z.-G.; Sun, Z.-R.; Lang, J.-P. *Chem. Commun.* **2013**, *49*, 4836. (c) Li, Y.-J.; Latouche, C.; Kahlal, S.; Liao, J.-H.; Dhayal, R. S.; Saillard, J.-Y.; Liu, C. W. *Inorg. Chem.* **2012**, *51*, 7439. (d) Li, B.; Liao, J.-H.; Tang, H.-T.; Li, Y.-J.; Liu, C. W. *Dalton Trans.* **2013**, *42*, 14384. (e) Gonzalez-Duarte, P.; Clegg, W.; Casals, I.; Sola, J.; Rius, J. *J. Am. Chem. Soc.* **1998**, *120*, 1260. (f) Sachse, A.; Demeshko, S.; Meyer, F. *Dalton Trans.* **2009**, 7756. (g) Wang, Q.-M.; Mak, T. C. W. *Chem. Commun.* **2000**, 1435. (h) Hezel, F.; Fenske, D.; Eisenmann, J.; Wetzel, T. *Z. Anorg. Allg. Chem.* **2000**, *626*, 290. (i) Burgi, H. B.; Gehrer, H.; Strickler, P.; Winkler, F. K. *Helv. Chim. Acta* **1976**, *59*, 2558.

(12) (a) Liu, C. W.; Hung, C.-M.; Santra, B. K.; Chu, Y.-H.; Wang, J.-C.; Lin, Z. *Inorg. Chem.* **2004**, *43*, 4306. (b) Liu, C. W.; Sarkar, B.; Huang, Y.-J.; Liao, P.-K.; Wang, J.-C.; Saillard, J.-Y.; Kahlal, S. *J. Am. Chem. Soc.* **2009**, *131*, 11222. (c) Liu, C. W.; Haia, H.-C.; Hung, C.-M.; Santra, B. K.; Liaw, B.-J.; Lin, Z.; Wang, J.-C. *Inorg. Chem.* **2004**, *43*, 4464. (d) Latouche, C.; Kahlal, S.; Furet, E.; Liao, P.-K.; Lin, Y.-R.; Fang, C.-S.; Cuny, J.; Liu, C. W.; Saillard, J.-Y. *Inorg. Chem.* **2013**, *52*, 7752. (e) Liu, C. W.; Chang, H.-W.; Fang, C.-S.; Sarkar, B.; Wang, J.-C. *Chem. Commun.* **2010**, *46*, 4571.

(13) (a) Garland, M. T.; Halet, J.-F.; Saillard, J.-Y. *Inorg. Chem.* **2001**, *40*, 3342. (b) Zouchoune, B.; Ogliaro, F.; Halet, J.-F.; Saillard, J.-Y. *Inorg. Chem.* **1998**, *37*, 865. (c) Dhayal, R. S.; Liao, J. H.; Lin, Y. R.; Liao, P. K.; Kahlal, S.; Saillard, J. Y.; Liu, C. W. *J. Am. Chem. Soc.* **2013**, *135*, 4704.

(14) Rais, D.; Mingos, D. M. P.; Vilar, R.; White, A. J. P.; Williams, D. J. *J. Organomet. Chem.* **2002**, *652*, 87.

(15) Galbraith, J. M. *J. Chem. Educ.* **2007**, *84*, 783.

(16) (a) Liu, C. W.; Fang, C. S.; Fu, R. J.; Chang, H. W.; Saillard, J. Y.; Kahlal, S.; Wang, J. C.; Chang, I. J. *Inorg. Chem.* **2010**, *49*, 4934. (b) Latouche, C.; Liu, C. W.; Saillard, J.-Y. *J. Cluster. Sci.* **2014**, *25*, 147.

(17) Perrin, D. D.; Armarego, W. L. F.; Perrin, D. R. *Purification of Laboratory Chemicals*, 2nd ed.; Pergamon Press: Oxford, 1980.

(18) Rauhut, M. M.; Currier, H. A.; Wystrach, V. P. *J. Org. Chem.* **1961**, *26*, 5133.

(19) Included in *SAINT V4.043: Software for the CCD detector system*; Bruker Analytical: Madison, WI, 1995.

(20) Sheldrick, G. M. *SHELXL-97: Program for the refinement of crystal structure*; University of Göttingen: Göttingen, Germany, 1997.

(21) *SHELXL 5.10 (PC Version): Program Library for Structure Solutionand Molecular Graphics*; Bruker Analytical: Maidson, WI, 1998.

(22) Frisch, M. J.; Trucks, G. W.; Schlegel, H. B.; Scuseria, G. E.; Robb, M. A.; Cheeseman, J. R.; Scalmani, G.; Barone, M. V.; Petersson, G. A.; Nakatsuji, H.; Caricato, M.; Li, X.; Hratchian, H. P; Izmaylov, A. F.; Bloino, J.; Zheng, G.; Sonnenberg, J. L.; Hada, M.;

Ehara, M.; Toyota, K.; Fukuda, R.; Hasegawa, J.; Ishida, M.; Nakajima, T.; Honda, Y.; Kitao, O.; Nakai, H.; Vreven, T.; Montgomery, J. A. J.; Peralta, J. E.; Ogliaro, F.; Bearpark, M.; Heyd, J. J.; Brothers, E.; Kudin, K. N.; Staroverov, V. N.; Kobayashi, R.; Normand, J.; Raghavachari, K.; Rendell, A.; Burant, J. C.; Iyengar, S. S.; Tomasi, J.; Cossi, M.; Rega, N.; Millam, J. M.; Klene, M.; Knox, J. E.; Cross, J. B.; Bakken, V.; Adamo, C.; Jaramillo, J.; Gomperts, R.; Stratmann, R. E.; Yazyev, O.; Austin, A. J.; Cammi, R.; Pomelli, C.; Ochterski, J. W.; Martin, R. L.; Morokuma, K.; Zakrzewski, V. G.; Voth, G. A.; Salvador, P.; Dannenberg, J. J.; Dapprich, S.; Daniels, A. D.; Farkas, Ö.; Foresman, J. B.; Ortiz, J. V.; Cioslowski, J.; Fox, D. J. *Gaussian 09*, rev. A.1; Gaussian Inc., Wallingford, CT, 2009.

(23) Weigend, F.; Ahlrichs, R. *Phys. Chem. Chem. Phys.* **2005**, *7*, 3297.

(24) (a) Becke, A. D. *Phys. Rev. A* **1988**, *38*, 3098. (b) Perdew, J. P. *Phys. Rev. B* **1986**, *33*, 8822.

(25) Zhao, Y.; Truhlar, D. G. *Theor. Chem. Acc.* **2008**, *120*, 215.

(26) Zhao, Y.; Truhlar, D. G. *J. Chem. Phys.* **2006**, *125* (194101), 1.

(27) (a) Adamo, C.; Barone, V. *J. Chem. Phys.* **1999**, *110*, 6158. (b) Ernzerhof, M.; Scuseria, G. E. *J. Chem. Phys.* **1999**, *110*, 5029.

(28) Grimme, S. *J. Comput. Chem.* **2006**, *27*, 1787.

(29) Glendening, E. D.; Badenhoop, J. K.; Reed, A. E.; Carpenter, J. E.; Bohmann, J. A.; Morales, C. M.; Weinhold, F. *NBO 5.0*; Theoretical Chemistry Institute, University of Wisconsin, Madison, WI, 2001; http://www.chem.wisc.edu/~nbo5.

(30) Gorelsky, S. I. *AOMix: Program for Molecular Orbital Analysis*, 2009; www.sg-chem.net.

(31) (a) Hay, P. J.; Wadt, W. R. *J. Chem. Phys.* **1985**, *82*, 270. (b) Hay, P. J.; Wadt, W. R. *J. Chem. Phys.* **1985**, *82*, 284. (c) Hay, P. J.; Wadt, W. R. *J. Chem. Phys.* **1985**, *82*, 299. (d) Schafer, A.; Hom, H.; Ahlrichs, R. *J. Chem. Phys.* **1992**, *97*, 2571.